The current issue and full text archive of this journal is available at
www.emeraldinsight.com/0961-5539.htm

Transient moment to rotate inner walls of vertical concentric annuli in the natural convection regime

Maged A.I. El-Shaarawi and Ali A. Al-Ugla
Mechanical Engineering Department, King Fahd University of Petroleum and Minerals, Dhahran, Saudi Arabia

Received 20 November 2007
Accepted 28 January 2008

Abstract

Purpose – The paper seeks to focus on obtaining the transient torque required to rotate the inner cylinder in open ended vertical concentric annuli for a fluid of $Pr = 0.7$ in the laminar natural convection flow regime over a wide range of the controlling parameter Gr^2/Ta. The inner wall is heated and subjected to an impulsive rotation while the outer one is stationary and maintained adiabatic.

Design/methodology/approach – The governing transient boundary-layer equations are numerically solved using an iterative linearized finite-difference scheme.

Findings – The transient induced flow rate and absorbed heat for different annulus heights are presented. High rotational speed (i.e. low values of Gr^2/Ta) increases the flow rate and heat absorbed in short annuli. However, for considerably tall annuli, Gr^2/Ta has slight effect on the flow and heat absorbed. The steady-state time is tangibly influenced by Gr^2/Ta in considerably short annuli and very slightly affected for considerably tall annuli.

Practical implications – The investigated problem can simulate the start-up period of naturally cooled small vertical electric motors.

Originality/value – The paper presents results not available in the literature for the effect of Gr^2/Ta on the developing velocities, pressure, flow-rate induced, absorbed heat by fluid and required torque in vertical concentric annuli with impulsively rotated inner walls under the transient free-convection heat transfer mode.

Keywords Convection, Rotational motion, Torque
Paper type Research paper

Nomenclature

b	annular gap width, $(r_2 - r_1)$
C_p	specific heat of fluid at constant pressure
D	equivalent (hydraulic) diameter of the annulus, 2b
f	volumetric flow rate, $\int_{r_2}^{r_2} 2\pi r u dr = \pi(r_2^2 - r_1^2)u_o$
F	dimensionless volumetric flow rate, $f/\pi 1 \nu Gr^* = (1 - N^2)U_o$
g	gravitational body force per unit mass (acceleration)
Gr	Grashoff number, $g\beta(T_w - T_o)D^3/\nu^2$
Gr*	modified Grashoff number, Gr(D/1)
h	heat gained by fluid from the entrance up to a particular elevation in the annulus, $\rho_o f C_p(T_m - T_o)$
$\overline{h}$	heat gained by fluid from the entrance up to the annulus exit, $\rho_o f c_p(\overline{T_m} - T_o)$
H	dimensionless heat absorbed from the entrance up to any particular elevation, $h/[\pi\rho_O C_p 1\gamma Gr^*(T_w - T_o)] = F\theta_m = 2\int_N^1 UR\theta \, dR$
$\overline{H}$	dimensionless heat absorbed from the entrance up to the annulus exit $Z=L$, $\overline{h}/[\pi\rho_O C_p 1\gamma Gr^*(T_w - T_o)] = F\overline{\theta_m} = 2\int_N^1 UR\theta dR$
1	height of annulus

International Journal of Numerical Methods for Heat & Fluid Flow
Vol. 19 No. 2, 2009
pp. 201-222

0961-5539
DOI 10.1108/09615530910930973

L	dimensionless height of annulus, 1/Gr*
M*	torque (moment) required to rotate the inner cylinder
M	dimensionless torque, $M^*/2\rho\pi r_1^3 r_2 \Omega u_o$
N	radius ratio, r_1/r_2
p	Pressure of the fluid inside the channel at any cross station
p′	pressure defect at any point, $p - p_s$
p_o	pressure of the fluid at the annulus entrance, $-(\rho_O u_o^2/2)$
p_s	hydrostatic pressure, $-\rho_o g z$
P	dimensionless pressure defect at any point, $p' r_2^4/\rho_O 1^2 \gamma^2 (Gr^*)^2$
P_o	dimensionless pressure defect at the annulus entrance, $p_o r_2^4/\rho_O 1^2 \gamma^2 (Gr^*)^2 = -U_o^2/2$
P_{iw}	dimensionless pressure defect at the inner wall
P_{ow}	dimensionless pressure defect at the outer wall
Pr	Prandtl number, $\mu C_p/\kappa = \gamma/\alpha$
r	radial coordinate
r_1	inner radius of the annulus
r_2	outer radius of the annulus
R	dimensional radial coordinate, r/r_2
t	dimensionless time, $\nu t * /r_2^2$
θ	dimensionless temperature, $(T - T_O)/(T_w - T_O)$
T_o	fluid temperature at annulus entrance
T_w	temperature of heat transfer boundary
T_m	dimensionless mixing cup temperature
Ta	Taylor number, $2\Omega^2 r_1^2 b^3/(\gamma^2(r_1 + r_2))$
Ta*	modified Taylor number, $Ta(b/l)^2$
u	instantaneous axial velocity component at any point
u_o	instantaneous entrance axial velocity, $\int_{r_1}^{r_2} 2\pi r u \mathrm{d}r/[\pi(r_2^2 - r_1^2)]$
U	dimensionless axial velocity component at any point, $ur_2^2/1\gamma Gr*$
U_o	dimensionless axial velocity at the entrance, $u_o r_2^2/1\gamma Gr*$
v	radial velocity component at any point
V	dimensionless radial velocity component at any point, $\rho v r_2/\mu$
w	instantaneous tangential velocity component at any point
W	dimensionless tangential velocity component at any point, $w/\Omega_1 r_1$
z	axial coordinate
Z	dimensionless axial coordinate, $z/1Gr*$
α	thermal diffusivity, $\kappa/\rho_o C_p$
β	coefficient of thermal expansion
ν	kinematic fluid viscosity, μ/ρ_o
Ω	angular velocity of the inner wall
ρ	fluid density
μ	dynamic fluid viscosity
τ^*	tangential shear stress on the inner cylinder surface, $\mu(\partial w/\partial r)_{r_1}$
τ	dimensionless tangential shear stress on the inner cylinder surface, $(\tau^*/\mu\Omega N) = (\partial W/\partial R_{R=N})$

Introduction

Unsteady free convection flow between concentric cylinders has many applications in convection heat transfer devices and electric machines. The transfer of heat by natural convection is always a factor in the cooling of electric machines. The design of cooling

systems for such electric machines requires knowledge of the hydrodynamic behavior of the flow to limit the rotor temperature to less than the maximum permitted value.

The transient nature on flows may be caused by many reasons. One of such reasons is due to the sudden starting that takes place at the early stages of operating any machine. A very important application pertaining to this research is the starting of the naturally cooled electric motors. Beside other applications in chemical mixings processes, fiber coating applications and drying machinery, there are possibilities of future applications for compact rotary heat exchangers and combustion chambers.

Literature up to 1982 for the flow between parallel plates can be found in Nakamura *et al.* (1982). Joshi (1988) studied the transient natural convection between vertical parallel plates numerically. The two classical boundary conditions of uniform wall temperature and uniform heat flux were considered. His results presented the rate of heat transfer for uniform wall temperature and the maximum wall temperature for uniform heat flux. Nelson and Wood (1989) presented a numerical analysis for developing laminar flow between vertical parallel plates for combined heat and mass transfer natural convection with uniform wall temperature and concentration boundary condition. They found that at intermediate Rayleigh numbers, the parallel plate heat and mass transfer is higher than that for single plate. Floryan and Novak (1994) investigated the free convection heat transfer in multiple parallel vertical channels with isothermal walls. Their results show that the interaction between channels increases with Grashoff number and decreases with the distance between them. Al-Subaie and Chamkha (2003) developed an analytical solution for the continuum equations governing transient, laminar, fully developed natural convection flow of a particulate suspension through an infinitely long vertical channel.

Flow in stationary vertical annuli and cylinders have been reported in the following references (Hess and Miller, 1979; Prasad *et al.*, 1986; Holzbecher and Steiff, 1995; Zaki *et al.*, 2000; Al-Arabi *et al.*, 1987; Rogers and Yao, 1993; Kumar, 1997; El-Shaarawi and Negm, 1999; El-Shaarawi and Al-Nimr, 1990; El-Shaarawi and Alkam, 1992; El-Shaarawi and Al-Attas, 1992; El-Shaarawi *et al.*, 1995, 1999; Reeve *et al.*, 2004). Experimental investigations have been focused in the following references (Hess and Miller, 1979; Prasad *et al.*, 1986; Holzbecher and Steiff, 1995; Zaki *et al.*, 2000). Hess and Miller (1979) investigated experimentally the axial velocity of fluid contained in a cylinder subject to constant heat flux. They used a laser Doppler velocimeter to measure this velocity. They showed that the flow field is different from that on a vertical flat plate due to recirculating zone and the presence of the top. Prasad *et al.* (1986) studied experimentally the steady-state natural convection in a concentric tall vertical annulus filled with saturated porous media when the inner wall is heated by applying a constant heat flux and the outer wall is isothermally cooled. They obtained the temperature profiles and heat transfer rates for the two aspects and radius ratios of 14.4 and 11.08. Holzbecher and Steiff (1995) investigated experimentally the natural convection flow in internally heated vertical cylinders. Zaki *et al.* (2000) studied the natural convection mass transfer behavior of the inner cylinder of a long vertical annulus by measuring the limiting current of the cathodic deposition of copper from acidified copper sulphate solution.

Numerical investigations for developing steady free convection in vertical concentric annuli can be found in the following references (Al-Arabi *et al.*, 1987; Rogers and Yao, 1993; Kumar, 1997; El-Shaarawi and Negm, 1999). Al-Arabi *et al.* (1987) used a finite-difference method to study the laminar natural convection through vertical annuli with one wall uniformly heated and the other wall adiabatic. Rogers and Yao

(1993) studied the natural convection in a heated vertical concentric annulus with constant heat flux on the inner cylinder and the outer cylinder is insulated. Their results show that the instability occurrence is dependent on the Prandtl number. Kumar (1997) obtained numerical results of heat transfer rates and flow fields in a vertical annulus with longitudinal fins for various parameters. He found that the heat transfer rate increases as the fin ratio and the radius ratio increase. Also, the heat transfer rate decreases as the aspect ratio and the fin thickness increase. El-Shaarawi and Negm (1999) presented the steady conjugate heat transfer problem in vertical open-ended concentric annuli under the laminar natural convection flow regime. They used a finite-difference technique to solve the governing equations with the outer wall being isothermal while the inner wall is kept adiabatic. They presented effect of solid–fluid conductivity ratio on the induced flow behavior and other engineering parameters. Fully-developed natural convection has been investigated by El-Shaarawi and Al-Nimr (1990). They presented the analytical solutions for fully developed natural convection in open-ended vertical concentric annuli corresponding to four fundamental boundary conditions. They presented the volumetric flow rate, heat absorbed, fluid temperature and local Nusselt number.

Transient convection heat transfer in vertical concentric annuli has been treated in the following references (El-Shaarawi and Alkam, 1992; El-Shaarawi and Al-Attas, 1992; El-Shaarawi *et al.*, 1995, 1999; Reeve *et al.*, 2004). El-Shaarawi and Alkam (1992) used a finite-difference scheme to solve the transient laminar forced convection problem in the entry region of a concentric annulus with a step change in temperature at one of the annulus boundaries or a step change in temperature at both inlet cross-section and one of annulus boundaries while the other boundary kept adiabatic. They found that heating outer boundary effect is much higher than heating the inner boundary. El-Shaarawi and Al-Attas (1992) investigated the transient laminar free-convection problem in vertical open-ended concentric annuli. El-Shaarawi *et al.* (1995) used finite-difference scheme to solve the transient conjugate heat transfer problem in concentric annuli. They showed the effects of solid-fluid conductivity ratio and diffusivity ratio on the thermal behavior of the flow. El-Shaarawi *et al.* (1999) investigated numerically the transient conjugate heat transfer in a porous medium in concentric annuli. Reeve *et al.* (2004) presented the numerical predictions of axisymmetric natural convection within a tall annular cavity with an aspect ratio of 10 and radius ratio of 0.6.

Flow between concentric annuli with the inner wall rotating has been studied in the following papers. Bird *et al.* (1959) obtained the pressure distribution for isothermal, pure tangential flow in an annulus by first solving for a compressible fluid and then taking the limit as the deviation from the incompressibility vanishes. They obtained an analytical expression for pressure vs the radial coordinate for either or both cylinder in rotation. El-Shaarawi and Sarhan (1981) developed a finite-difference scheme for solving the boundary-layer equations governing the laminar free convection flow in open-ended vertical concentric annuli with rotating inner walls with one wall being isothermal and the other wall adiabatic. El-Shaarawi and Khamis (1987) investigated the laminar induced flow natural convection through an open-ended vertical annulus with a rotating inner cylinder heated at constant heat flux and an adiabatic outer boundary. They used finite-difference scheme to solve the boundary-layer governing equations. El-Shaarawi *et al.* (1997) studied numerically the tangential shear stress and the torque required to turn the inner shaft of concentric annuli having laminar forced flow with simultaneously developing tangential and axial boundary layers. They presented the effect of the two controlling parameters (radius ratio (N) and Re^2/Ta) on the torque. Hwang and Yang

(2004) studied numerically the flow between two concentric cylinders with inner one rotating and with imposed pressure-driven axial flow. They found that the axial flow stabilizes the flow field and decreases the torque required to rotate the inner cylinder at a given speed. Kim and Choi (2005) analyzed using the linear theory the onset of initial instability in a developing Couette flow following the impulsive starting of an inner rotating cylinder. Ball *et al.* (1989) studied experimentally the convection flows engendered within the annular gap between concentric vertical cylinders with rotating and heated inner cylinder while the outer cylinder is stationary and cooled. Their results showed the interdependence between the heat transfer mechanism and the structure of the secondary flows. Mixed convection in vertical concentric annulus with the inner wall rotating has been investigated by El-Shaarawi and Sarhan (1982). They used finite-difference scheme to solve the combined forced-free laminar boundary layer flow in a vertical concentric annulus with a rotating inner cylinder. They investigated the effect of a superimposed aiding or opposing free convection on the developing tangential velocity profiles. Bird and Curtiss (1959) obtained an exact solution for the equations of the unsteady, laminar, tangential flow of isothermal fluid in the annular space between two cylinders one or both of which may be rotating. Mullin *et al.* (1981) measured the fluctuating cellular flows between concentric cylinders with the inner one rotating using the recurrence-rate correlation technique.

Governing equations

Figure 1 shows a concentric annulus and the cylindrical coordinate system used. Initially, the fluid is at rest everywhere. Then a step rise in the temperature of the inner wall occurs simultaneously with an impulsive rotation of the inner wall. As a result of the step rise in the temperature, fluid rises in the annular gap between the cylindrical walls by natural convection. It is assumed that the fluid enters the annular gap with a time-dependent uniform velocity profile $u_o(t)$ of a value equal to the instantaneous mean axial velocity in the annular gap while the impulsively-rotated inner wall has a constant angular velocity, ω and the outer wall is stationary. Thus, the flow regime is

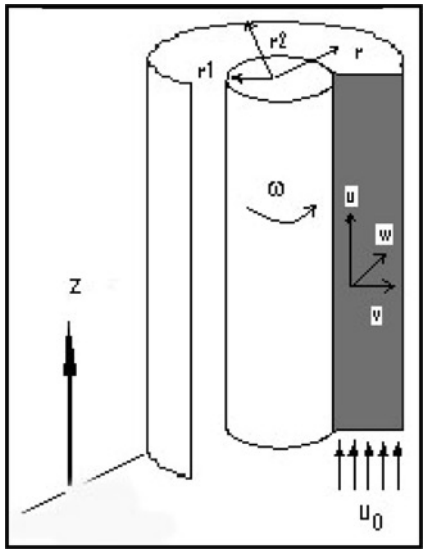

Figure 1.
Problem Geometry of the concentric cylinder and velocity components

an unsteady free convection flow through an annulus with an impulsively rotated inner wall with a constant angular velocity ω.

The fluid is assumed to be Newtonian, incompressible and has constant physical properties with the exception of the density that varies according to the Boussinesq approximation.

Under the above assumptions and using the boundary-layer simplifications (El-Shaarawi and Sarhan, 1981; El-Shaarawi *et al.*, 1997), the governing equations for the unsteady free convection in the entry region of a vertical concentric annulus with an impulsively rotating inner cylinder reduce to the following equations

$$\frac{1}{\mathrm{r}}\frac{\partial}{\partial \mathrm{r}}(\mathrm{rv}) + \left(\frac{\partial \mathrm{u}}{\partial \mathrm{z}}\right) = 0 \tag{1}$$

$$\rho_O\left(\frac{w^2}{r}\right) = \left(\frac{\partial P}{\partial r}\right) \tag{2}$$

$$\rho_O\left(\frac{\partial w}{\partial t} + v\frac{\partial w}{\partial r} + u\frac{\partial w}{\partial z}\right) = \mu\left(\frac{\partial^2 w}{\partial r^2} + \frac{1}{r}\frac{\partial w}{\partial r} - \frac{w}{r^2}\right) \tag{3}$$

$$\frac{\partial u}{\partial t^*} + v\frac{\partial u}{\partial r} + u\frac{\partial u}{\partial z} = -\frac{1}{\rho_O}\frac{\partial p}{\partial z} + g\beta(T - T_O) + \frac{\nu}{r}\frac{\partial}{\partial r}\left(r\frac{\partial u}{\partial r}\right) \tag{4}$$

$$\frac{\partial T}{\partial t^*} + v\frac{\partial T}{\partial r} + u\frac{\partial T}{\partial z} = \frac{\alpha}{r}\frac{\partial}{\partial r}\left(r\frac{\partial T}{\partial r}\right) \tag{5}$$

Introducing the dimensionless parameters given in the Appendix, these equations can be written as follows

$$\frac{\partial V}{\partial R} + \frac{V}{R} + \frac{\partial U}{\partial Z} = 0 \tag{6}$$

$$\frac{W^2}{R} = \frac{8(1-N)^5}{1+N}\frac{\mathrm{Gr}^2}{\mathrm{Ta}}\frac{\partial P}{\partial R} \tag{7}$$

$$\frac{\partial W}{\partial t} + V\frac{\partial W}{\partial R} + U\frac{\partial W}{\partial Z} = \frac{\partial^2 W}{\partial R^2} + \frac{1}{R}\frac{\partial W}{\partial R} - \frac{W}{R^2} \tag{8}$$

$$\frac{\partial U}{\partial t} + V\frac{\partial U}{\partial R} + U\frac{\partial U}{\partial Z} = -\frac{\partial P}{\partial Z} + \frac{\theta}{16(1-N)^4} + \frac{1}{R}\frac{\partial}{\partial R}\left(R\frac{\partial U}{\partial R}\right) \tag{9}$$

$$\frac{\partial \theta}{\partial t} + V\frac{\partial \theta}{\partial R} + U\frac{\partial \theta}{\partial Z} = \frac{1}{\mathrm{Pr}}\frac{1}{R}\frac{\partial}{\partial R}\left(R\frac{\partial \theta}{\partial R}\right) \tag{10}$$

These five coupled equations (Equations (6)-(10)) are subject to the following initial and boundary conditions

Initial conditions ($t = 0$): $U = V = W = P = \theta = 0$ everywhere

For $t > 0$:

Entrance conditions: At $Z = 0$ and $N < R < 1$, $U = U_o(t)$, $V = W = \theta = 0$ and $P = -U_o^2/2$

Inner wall conditions: For $Z > 0$ and $R = N$: $U = V = 0$, $W = 1$, $\theta = 1$(isothermal inner wall)

Outer wall conditions: For $Z < 0$ and $R = 1$: $U = V = W = 0$, $\partial\theta/\partial R = 0$ (adiabatic outer wall)

Equation (6) subject to the above conditions can be written in the following integral form:

$$F = (1 - N^2)U_o = 2\int_N^1 RUdR \tag{11}$$

Results and discussion

The above equations have been numerically solved using an iterative linearized finite-difference scheme (El-Shaarawi and Alkam, 1992; El-Shaarawi *et al.*, 1995, 1997; El-Shaarawi and Sarhan, 1981). For an annulus of a given N, the numerical solution of the finite-difference equations is obtained by first selecting values of N, Gr^2/Ta, Pr, L (dimensionless annulus height, 1/Gr), ΔR , ΔZ and Δt. Moreover, for each time step, the value of the inlet velocity $U_o(t)$ should be assumed. Such an assumed value of $U_o(t)$ should give a value of the dimensionless pressure defect at the exit section equals zero or practically satisfies the arbitrarily chosen criterion close to zero ($\pm 10^{-15}$). To satisfy this condition, iteration process is used for every time step as follows. First, the inlet axial velocity (U_o) is assumed and computations continue, for this time step, till the exit-cross-section dimensionless pressure defect is obtained. If it does not satisfy the above criterion, another value of the inlet axial velocity has to be assumed, for the same time step, and its corresponding exit dimensionless pressure defect has to be computed. Then, a linear interpolation is done between these two assumed values of U_o to get the next trial value of the inlet axial velocity U_o corresponding to zero dimensionless pressure defect at the annulus exit. Such an interpolation process continues, for the same time step, till the dimensionless exit pressure defect satisfies the above iteration criterion.

The above numerical algorithm starts by the solution of the tangential momentum equation to obtain the values of W after one time step, Δt. Starting with $j = 1$ (annulus entrance cross-section) and applying the finite-difference form of Equation (8), we get simultaneous linear equations which when solved by Thomas' method give the unknown values of W's at all points of the second cross-section. Similarly, the temperature field is obtained by applying the finite-difference form of Equation (10) with to get the unknown values of θ's at the second cross-section when solved by Thomas' method. Now applying the finite-difference forms of Equation (9) together with Equation (11) we obtain equations which when solved by a special form of Gauss–Jordan eliminations scheme give the unknown values of U's at all points of the second cross-section and $P_{1,2,2}$. After getting $P_{1,2,2}$, the finite-difference form of Equation (7) can now be applied in a stepwise order with $i = 2, 3, \ldots, n + 1$ to get the values of

$P_{2,2,2,} \ldots, P_{n+1,2,2}$. Using the computed values of U's and applying the finite-difference form of Equation (6) we get the values of V's at all points of the second cross-section.

The same procedure process can then be repeated for each next time step till steady-state conditions are reached. The change in the total heat absorbed is used as a criterion for the achievement of steady-state conditions. Steady-state conditions are considered achieved if the following criterion is satisfied:

$$-10^{-6} \leq \frac{\overline{H}(k+1) - \overline{H}(k)}{\overline{H}(k+1)} \leq 10^{-6}.$$

Engineers are usually interested in calculating the torque required to rotate the inner cylinder. At a given axial distance from the annulus entrance (z), the infinitesimal resisting torque (dM*) exerted by the fluid on a surface element of the inner cylinder having an area $dA = 2\pi r_1 dz$ is due to the local tangential shear stress $\tau^* = \mu(\partial w/\partial r)_{r_1}$ and is given by

$$dM^* = 2\pi\mu r_1^2 \left(\frac{\partial w}{\partial r}\right)_{r_1} dz$$

Hence upon integration from the annulus entrance ($z = 0$) to any axial distance z, one obtains the following expression for the torque (M*) required to rotate a height z of the inner cylinder.

$$\mathrm{M}^* = 2\pi\mu r_1^2 \int_0^z \left(\frac{\partial w}{\partial r}\right)_{r_1} dz$$

Introducing the dimensionless torque (M) needed to rotate a dimensionless height Z as

$$\mathrm{M} = \frac{M^*}{\rho 2\pi r_1^3 r_2 \Omega u_{\mathrm{o}}}$$

Hence,

$$\mathrm{M} = \frac{2\pi\mu r_1^2 \int_0^z \left(\frac{\partial w}{\partial r}\right)_{r_1} dz}{\rho 2\pi r_1^3 r_2 \Omega u_o} = \frac{\mu \int_0^z \left(\frac{\partial w}{\partial r}\right)_{r_1} dz}{\rho r_1 r_2 \Omega u_o}$$

Using the dimensionless parameters given in the nomenclature, above equation can be written as

$$\mathrm{M} = \frac{\mu\Omega r_1 1 Gr^* \int_0^z \frac{\partial W}{\partial R_{R=N}} dZ}{\rho r_1 r_2^2 \Omega u_o} = \frac{\int_0^z \frac{\partial W}{\partial R_{R=N}} dZ}{U_o} \tag{12}$$

The total torque required to rotate the inner cylinder of height L, i.e. value of M at $Z = L$, is, therefore, given by

$$\mathrm{M}_{\mathrm{ex}} = \frac{\int_0^L \frac{\partial W}{\partial R_{R=N}} dZ}{U_o} \tag{13}$$

The steady-state fully-developed tangential and axial velocity profiles analytical solutions are given in El-Shaarawi and Sarhan (1981) as:

$$W_{ss,fd} = \frac{N}{1-N^2}\left[\frac{1}{R} - R\right] \tag{14}$$

$$U_{ss,fd} = \frac{1}{64(1-N)^4}\left[1 - R^2 - \frac{1-N^2}{\ln N} - \ln R\right] \tag{15}$$

To check the adequacy of the present numerical results, the steady-state fully developed tangential and axial velocity profiles which could be obtained at exit of a tall annulus at considerably large values of time have been compared in Table I with their corresponding analytical solution (given by Equations (14) and (15)).

R	Present results	W_{fd} Equation (14)	Percentage difference	Present results	U_{fd} Equation (15)	Percentage difference
0.600	0.71112808	0.71111111	0.00238595	0.02175052	0.02181895	0.31361429
0.700	0.48573286	0.48571429	0.00382474	0.03092045	0.03101753	0.31299564
0.800	0.30001428	0.30000000	0.00475877	0.02954585	0.02963848	0.31254839
0.900	0.14074834	0.14074074	0.00539895	0.01894010	0.01899942	0.31220640

Table I.
Comparison of the present steady-state fully-developed tangential and axial velocity values at the exit of a sufficiently tall annulus (L = 0.1) for $Gr^2/Ta = 500$ with the corresponding fully developed analytical solution

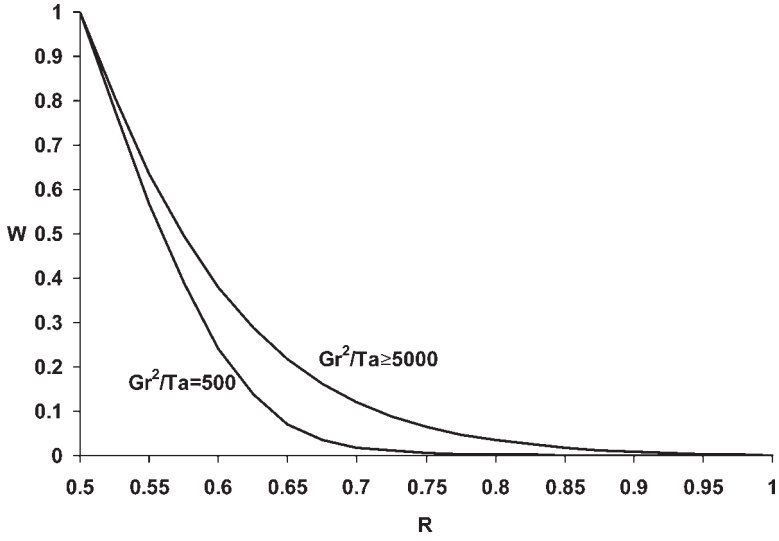

Figure 2.
Effect of Gr^2/Ta on the tangential velocity profiles at t = 0.01 for short annulus (L = 0.001) at Z = 0.0001 (near entrance)

To explore the physics of the transient flow, computations were carried out for a fluid of Pr = 0.7 in two annuli of N = 0.5 with L = 0.001 (short annulus) and L = 0.1 (tall annulus) at selected time and different values of Gr^2/Ta. Figures 2-4 and Table II show the effect of Gr^2/Ta on the developing tangential velocity profiles at specific values of time, t = 0.01 for a short annulus (L = 0.001) and t = 0.1 for a tall annulus (L = 0.1), at three different axial positions (near entrance, mid-height and exit). It can be seen that Gr^2/Ta has remarkable effects on the developing tangential velocity profiles in the short annulus as shown in Figures 2-4. However, for a tall annulus, Gr^2/Ta has a slight effect on the tangential velocity profiles near the entrance and such effect disappears from the mid-height till exit, as shown in Table II. The minimum value of Gr^2/Ta that was investigated for both annulus heights is 500. This is due to Taylor vortices that might occur with values of $Gr^2/Ta < 500$.

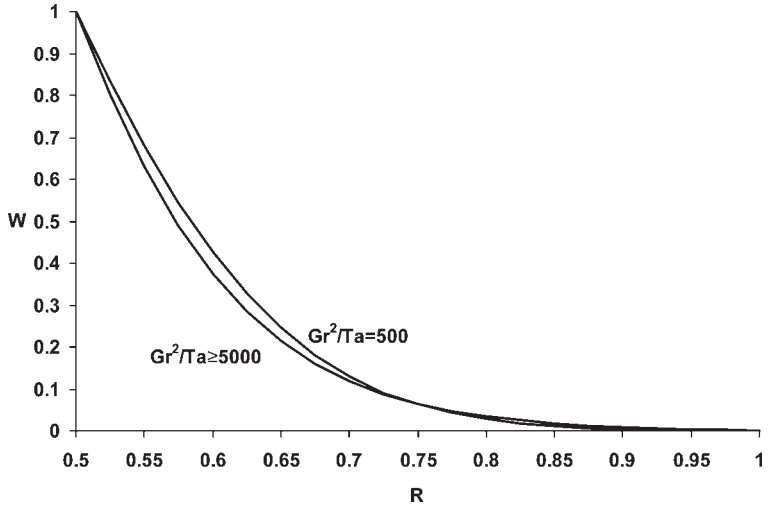

Figure 3.
Effect of Gr^2/Ta on the tangential velocity profiles at $t = 0.01$ for short annulus (L = 0.001) at Z = 0.0005 (mid-height)

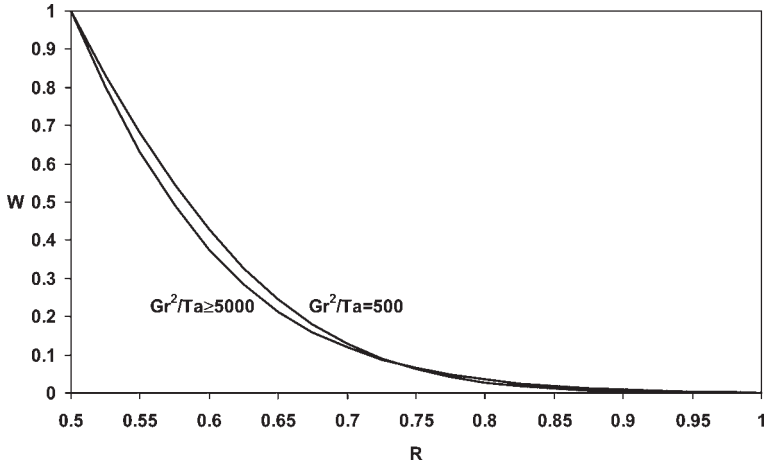

Figure 4.
Effect of Gr^2/Ta on the tangential velocity profiles at t = 0.01 for short annulus (L = 0.001) at Z = L (exit)

R	$Gr^2/Ta = 500$	$Gr^2/Ta = 5 \times 10^6$	Percentage difference	$Gr^2/Ta = 500$	$Gr^2/Ta = 5 \times 10^6$	Percentage difference
Values of W at Z = 0.0005 (near entrance)				*Values of W at Z = 0.05 (mid-height)*		
0.6	0.52059363	0.54307352	4.318126359	0.71029766	0.71029766	2.81347E-13
0.7	0.22322316	0.24559143	10.02058773	0.48448460	0.48448460	4.12480E-13
0.8	0.08768717	0.09945670	13.42218225	0.29884276	0.29884276	6.68713E-13
0.9	0.03201907	0.03652814	14.08245425	0.14006408	0.14006408	7.13388E-13
Values of W at Z = L (exit)						
0.6	0.71029766	0.71029766	1.40674E-13			
0.7	0.48448460	0.48448460	6.18720E-13			
0.8	0.29884276	0.29884276	1.02165E-12			
0.9	0.14006408	0.14006408	1.42678E-12			

Table II.
Effect of Gr^2/Ta on the tangential velocity at $t = 0.2$ for tall annulus ($L = 0.1$)

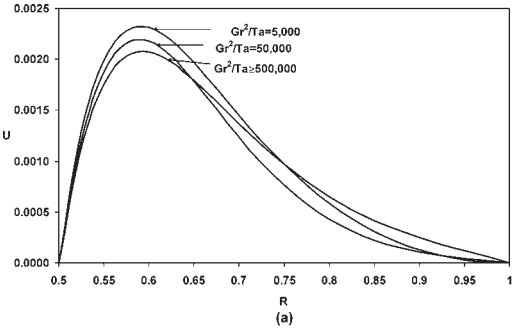

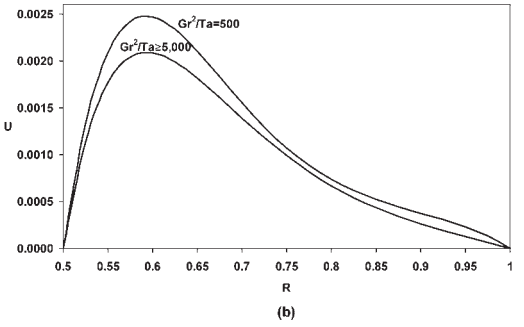

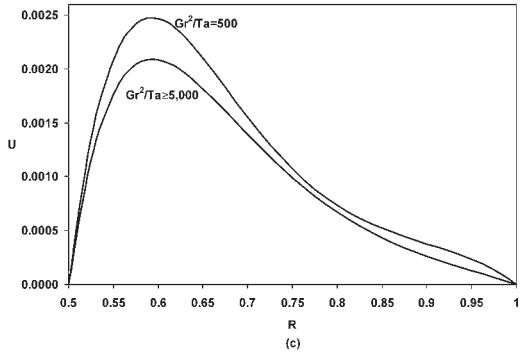

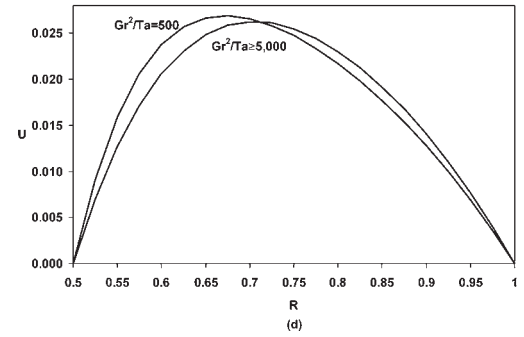

Figure 5.
(a) Effect of Gr^2/Ta on the axial velocity profiles at $t = 0.01$ for short annulus ($L = 0.001$) at $Z = 0.0001$ (near entrance); (b) effect of Gr^2/Ta on the axial velocity profiles at $t = 0.01$ for short annulus ($L = 0.001$) at $Z = 0.0005$ (mid-height); (c) effect of Gr^2/Ta on the axial velocity profiles at $t = 0.01$ for short annulus ($L = 0.001$) at $Z = L$ (exit); (d) effect of Gr^2/Ta on the axial velocity profiles at $t = 0.2$ for tall annulus ($L = 0.01$) at $Z = 0.0005$ (near entrance)

These figures show that for a given time and near the entrance the tangential velocity increases as Gr^2/Ta increases due to the thinning of the tangential boundary-layer thickness with the decrease in the value of Gr^2/Ta (i.e. the increase in the rotational speed of the inner cylinder for a given Gr, i.e. L). However, far away from the entrance in the short annulus ($L = 0.001$), the tangential velocity decreases as Gr^2/Ta increases as shown in Figures 3 and 4.

Figure 5(a)-(d) shows the effect of Gr^2/Ta on the axial velocity profiles in short and tall annuli. We can see that, for short annuli, decreasing Gr^2/Ta (increasing the inner cylinder rotational speed) generally increases the axial velocity at all axial positions (near entrance, mid-height, exit) and makes the axial velocity profiles more skewed inward. This is in agreement with Astill's results (Astill *et al.*, 1968) for the case of forced flow. However, for Gr^2/Ta more than 50,000 the axial velocity is not affected in both short and tall annuli.

On the other hand, for tall annuli Gr^2/Ta affects the axial velocity profiles only near entrance as shown in Figure 5(d) and Table III.

The effect of Gr^2/Ta on the radial pressure distribution at different axial positions for a given specific time values are presented in Figure 6(a)-(c). As Gr^2/Ta decreases (i.e. the rotational speed increases), the pressure decreases near the inner rotating wall for the two annulus heights at all the axial positions. However, for a considerably large value of $Gr^2/Ta \geq 50\times10^3$ (very low rotational speeds) the radial pressure becomes almost flat (showing no effect of the rotation on the radial velocity profile).

Figure 6(d)-(g) shows the variation of the pressure at the inner and outer walls of the annulus with the axial distance for short and tall annulus where $Gr^2/Ta = 10{,}000$ and 5,000, respectively. The pressure is lower at the inner wall than the outer wall due to the rotational speed effect as shown in the previous figures. The pressure decreases with time for both inner and outer walls and it decreases with Z after entrance then it recovers and increases with Z (as the buoyancy force develops and overcomes the friction force) until it reaches the atmospheric pressure at the outer wall of the exist cross-section.

Engineers are frequently not concerned with the velocity, pressure and temperature profiles. Rather they are interested in the torque needed to rotate the inner cylinder, the heat transferred to the fluid from the heated boundary and the induced flow rate through the annulus. Therefore, Figure 7(a)-(c) present the total torque (from entrance till the annulus exit) needed vs time for different annulus heights. As can be seen from these figures, the taller the annulus the higher the torque needed. For any given annulus height (L), torque decreases with time due to the sudden starting that takes place at the early stage and reaches the steady-state value at large value of time; the starting torque (at $t = 0$) is theoretically ∞ (due to the boundary-layer assumptions). Figure 7(a)-(c) are very useful for engineers to find the time variation of the power

R	Values of U at $Z = 0.05$ (mid-height) $Gr^2/Ta = 500$	$Gr^2/Ta = 5\times10^6$	Percentage difference	Values of U at $Z = L$ (exit) $Gr^2/Ta = 500$	$Gr^2/Ta = 5\times10^6$	Percentage difference
0.6	0.01837015	0.01830393	0.36043670	0.01837015	0.01830393	0.36043670
0.7	0.02560457	0.02551057	0.36710094	0.02560457	0.02551057	0.36710094
0.8	0.02412481	0.02403494	0.37250931	0.02412481	0.02403494	0.37250931
0.9	0.01534854	0.01529079	0.37625907	0.01534854	0.01529079	0.37625907

Table III.
Effect of Gr^2/Ta on the axial velocity at $t = 0.2$ for tall annulus ($L = 0.1$)

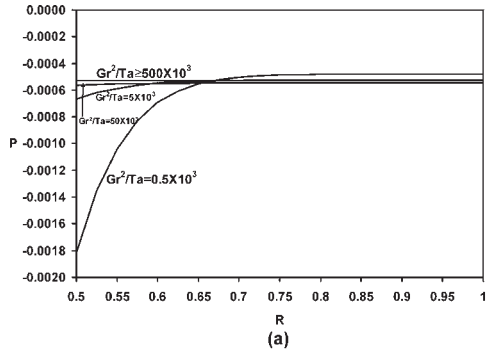

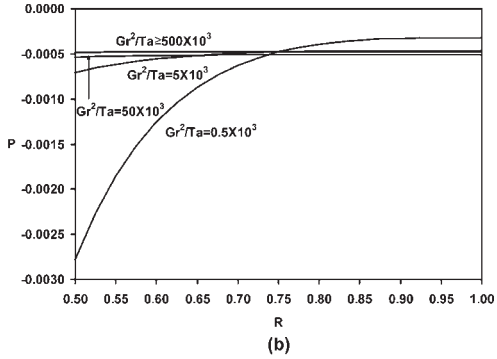

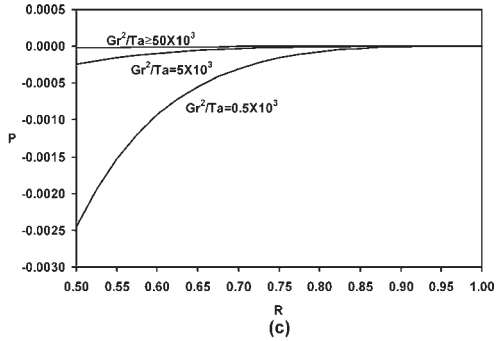

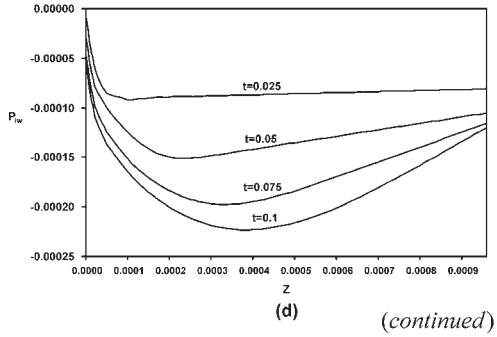

Figure 6.
(a) Effect of Gr^2/Ta on the pressure profiles at $t = 0.1$ for tall annulus ($L = 0.1$) at $Z = 0.0005$ (near entrance); (b) effect of Gr^2/Ta on the pressure profiles at $t = 0.1$ for tall annulus ($L = 0.1$) at $Z = 0.05$ (mid-height); (c) effect of Gr^2/Ta on the pressure profiles at $t = 0.1$ for tall annulus ($L = 0.1$) at $Z = L$ (exit); (d) pressure at the inner wall vs Z for short annuli ($L = 0.001$), $Gr^2/Ta = 10.000$; (e) pressure at the outer wall vs *Z* for short annuli ($L = 0.001$), $Gr^2/Ta = 10.000$; (f) pressure at the inner wall vs Z for tall annuli ($L = 0.1$), $Gr^2/Ta = 5,000$; (g) pressure at the outer wall vs Z for tall annuli ($L = 0.1$), $Gr^2/Ta = 5,000$

(*continued*)

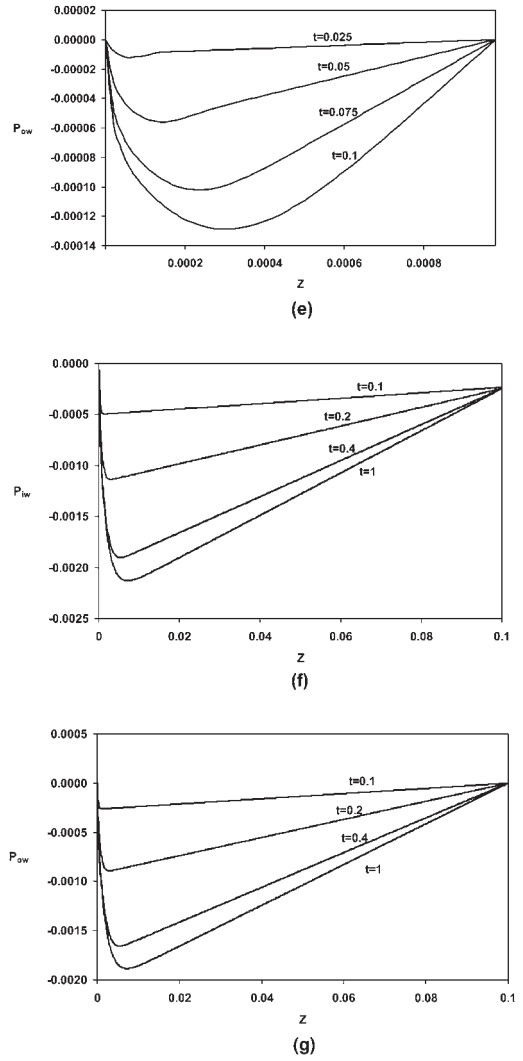

Figure 6.

needed to rotate the inner cylinder; the power is simply the torque multiplied by the rotational speed.

Figure 8(a)-(c) presents the volumetric flow rate vs time for various annulus heights. For a given time, the volumetric flow rate increases with height (L). Moreover, for a given annulus height the flow rate generally increases with time.

Figure 9(a) and (b) shows the total heat absorbed (H) vs time for the investigated values of annulus heights. As can be seen from these figures, the total heat, at a specific instant, is directly proportional to the annulus height (L). This is because as Gr* decreases (the annulus height increases) more flow is sucked by the annulus as a result of the chimney effect and hence more heat is absorbed by the fluid. The overshooting phenomenon is shown in these figures particularly for short annuli. It is clearly observed that the overshooting is more pronounced for short annuli than for tall annuli.

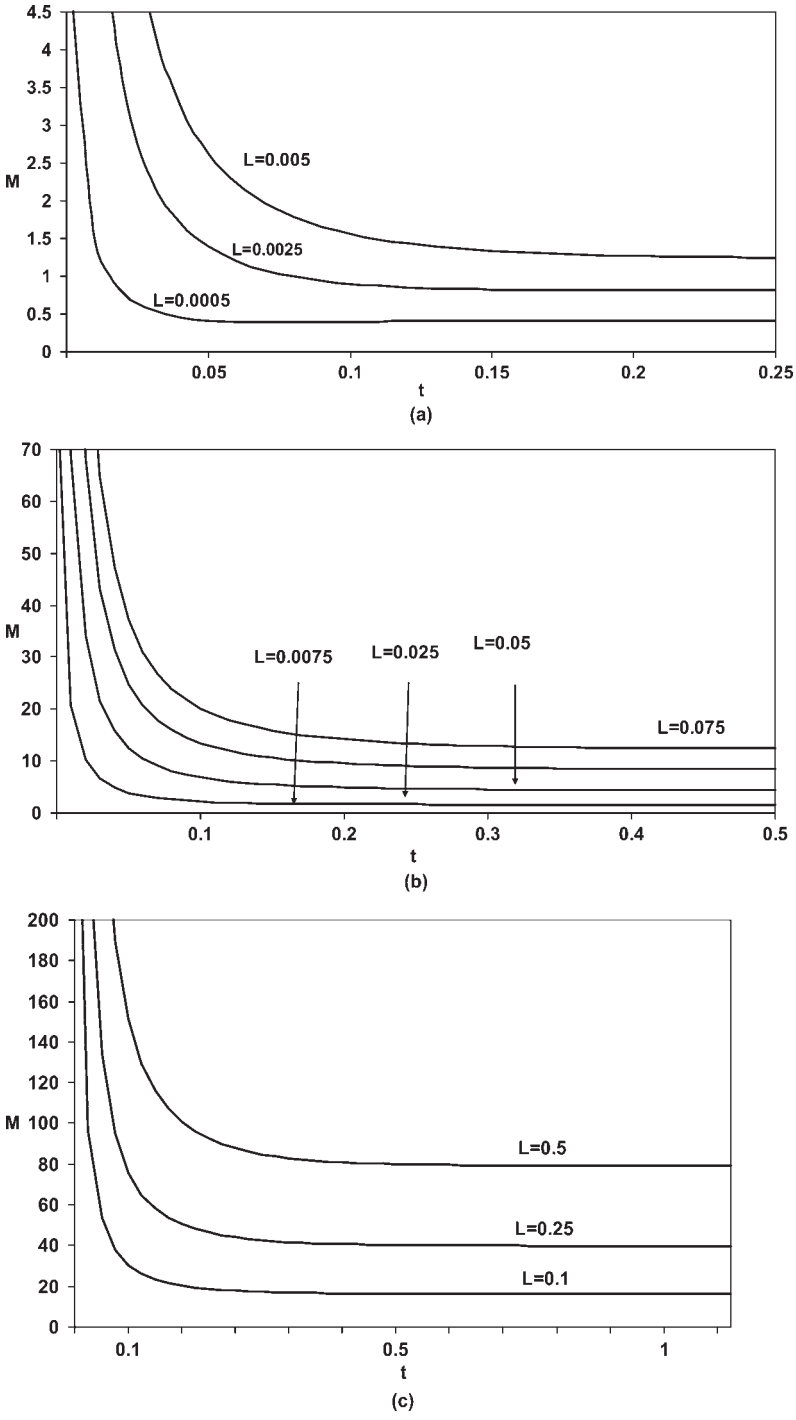

Figure 7.
(a) Total torque needed vs time ($0 \leq t \leq 0.25$), for different annulus heights, $0.0005 \leq L \leq 0.005$, $Gr^2/Ta = 50{,}000$; (b) total torque needed vs time ($0 \leq t \leq 0.5$), for different annulus heights, $0.0075 \leq L \leq 0.075$, $Gr^2/Ta = 50{,}000$; (c) total torque needed vs time ($0 \leq t \leq 1.0$), for different annulus heights, $0.1 \leq L \leq 0.5$, $Gr^2/Ta = 50{,}000$

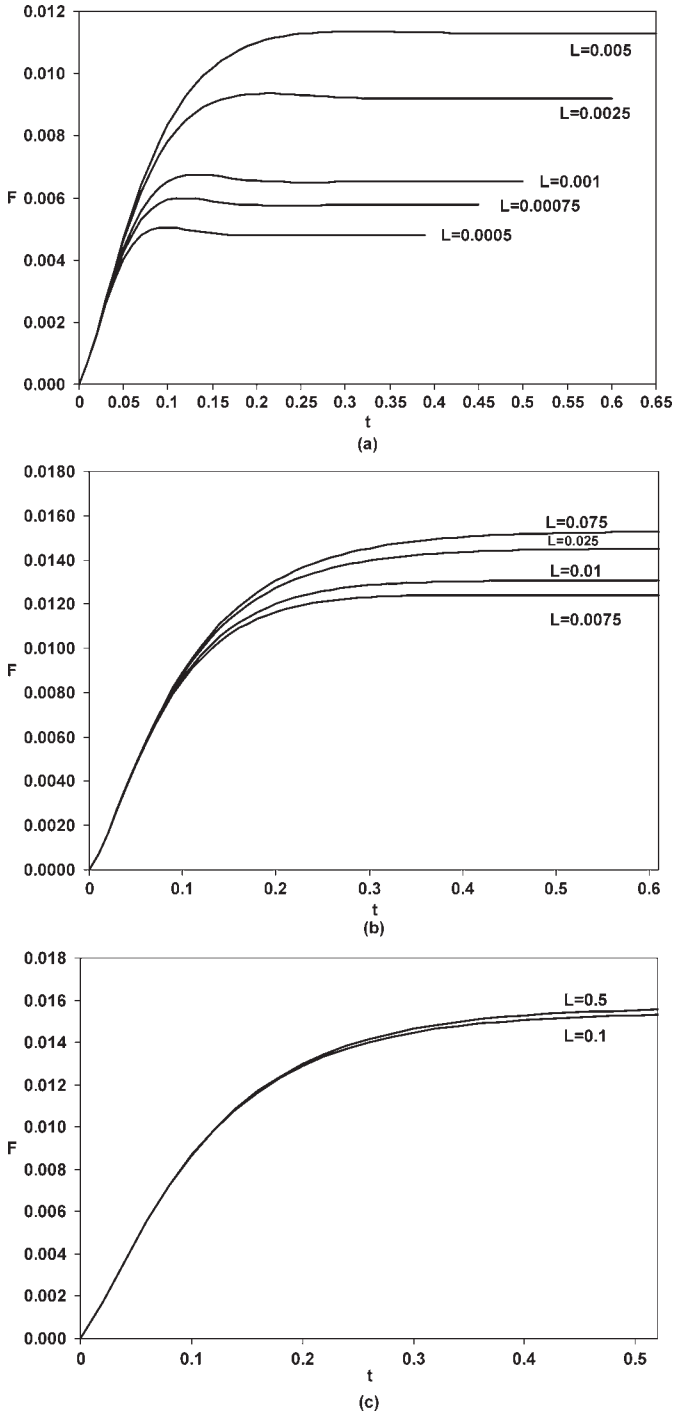

Figure 8.
(a) Flow rate (F) vs time $0.0005 \leq L \leq 0.005$, $Gr^2/Ta = 50{,}000$; (b) flow rate (F) vs time $0.0075 \leq L \leq 0.075$, $Gr^2/Ta = 50{,}000$; (c) flow rate (F) vs time $0.1 \leq L \leq 0.5$, $Gr^2/Ta = 50{,}000$

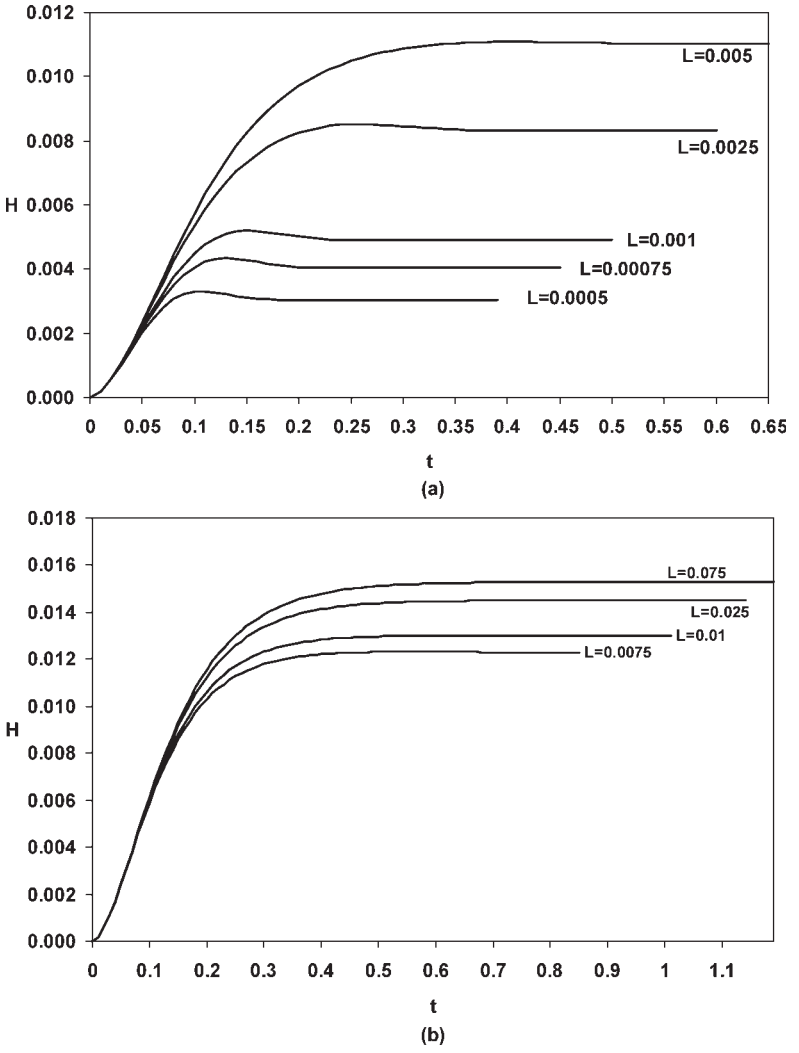

Figure 9.
(a) Total heat absorbed (H) vs time $0.0005 \leq L \leq 0.005$, $Gr^2/Ta = 50{,}000$; (b) Total heat absorbed (H) vs time $0.0075 \leq L = 0.075$, $Gr^2/Ta = 50{,}000$

		Flow rate			Heat absorbed		
	t	$Gr^2/Ta = 500$	$Gr^2/Ta = 5\times10^6$	Percentage difference	$Gr^2/Ta = 500$	$Gr^2/Ta = 5\times10^6$	Percentage difference
Table IV. Effect of Gr^2/Ta on the volumetric flow rate and heat absorbed for tall annulus ($L = 0.1$)	0.10	0.00868258	0.00864788	0.39966799	5.84E-03	5.81E-03	0.39589766
	0.20	0.01337921	0.01333084	0.36157630	1.13E-02	1.12E-02	0.36932372
	0.40	0.01511217	0.01506354	0.32183050	1.48E-02	1.48E-02	0.32183330
	0.80	0.01544828	0.01540019	0.31135487	1.54E-02	1.54E-02	0.31136761
	1.20	0.01545430	0.01540623	0.31108377	1.55E-02	1.54E-02	0.31105618

The rotational speed (hence Gr^2/Ta) has insignificant effect on either the volumetric flow rate or the heat absorbed for tall annuli ($L = 0.1$) as shown in Table IV. However, Figure 10(a) and (b) shows that for short annuli ($L = 0.001$) increasing the rotational speed (i.e. decreasing the value of Gr^2/Ta) induces higher flow rate and results higher heat absorbed.

The time needed to achieve the steady-state conditions (t_{ss}) is computed based on the criterion given in the method of solution. It is plotted against the annulus height in Figure 11. For a given value of Gr^2/Ta, the steady-state time (t_{ss}) increases with the annulus height. Similarly, for a given height, the steady-state time (t_{ss}) increases with Gr^2/Ta.

Finally, the results of this work show that the steady-state time for considerably short annuli reaches faster an almost constant value with Gr^2/Ta as shown in Table V.

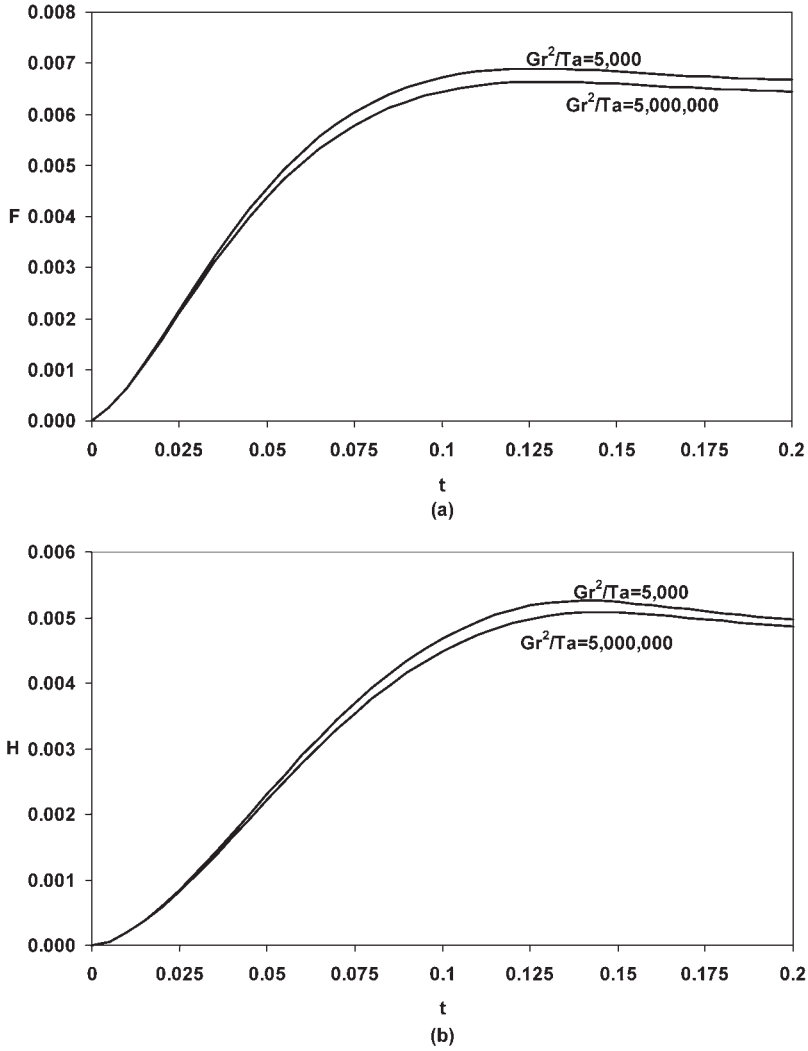

Figure 10.
(a) Effect of Gr^2/Ta on the volumetric flow rate for short annulus ($L = 0.001$); (b) effect of Gr^2/Ta on the heat absorbed for short annulus ($L = 0.001$)

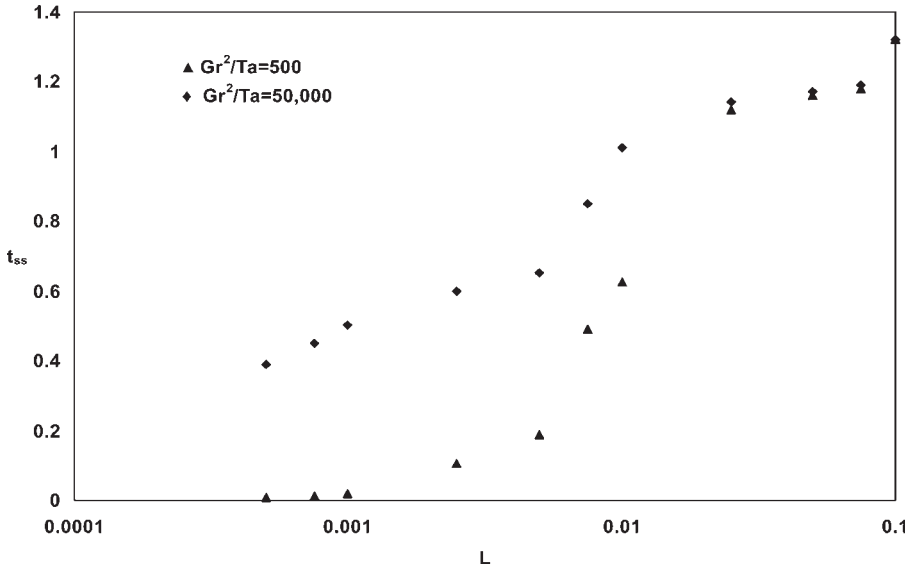

Figure 11.
Steady-state time vs annulus height, $Gr^2/Ta = 500$ and 50,000

Table V.
Steady-state time vs Gr^2/Ta for short annulus ($L = 0.001$)

Gr^2/Ta	500	5,000	500,000
t_{ss}	0.018	0.455	0.460

On the other hand, for considerably tall annuli ($L \geq 0.1$), there is almost no effect of the rotational speed (i.e. Gr^2/Ta) on the steady-state time values. For $L \geq 0.1$, the steady-state time value is 1.32 for all Gr^2/Ta values (over the range $500 \leq Gr^2/Ta \leq 5{,}000{,}000$).

Conclusions

This investigation provides data not available in the literature that are needed in many engineering applications for the effect of Gr^2/Ta on the developing velocities, pressure and torque in vertical concentric annuli under the transient free-convection heat transfer mode. Moreover, the transient induced flow rate and absorbed heat for different annulus heights have been presented.

The results show that high rotational speed (i.e. low values of Gr^2/Ta) increases the flow rate and heat absorbed in short annuli. However, for considerably tall annuli, Gr^2/Ta has slight effect on the flow and heat absorbed. Finally, the obtained results show that the steady-state time is tangibly influenced by Gr^2/Ta in considerably short annuli ($L = 0.001$) and very slightly affected for considerably tall annuli ($L \geq 0.1$).

References

Al-Arabi, M., El-Shaarawi, M. and Khamis, M. (1987), "Natural convection in uniformly heated vertical annuli", *International Journal of Heat and Mass Transfer*, Vol. 30, pp. 1381-90.

Al-Subaie, M.A. and Chamkha, A.J. (2003), "Transient natural convection flow of a particulate suspension through a vertical channel", *Heat and Mass Transfer*, Vol. 46, pp. 707-13.

Astill, K.N., Ganley, J.T. and Martin, B.W. (1968), "The developing tangential velocity profiles for axial flow in an annulus with a rotating inner cylinder", *Proceedings of the Royal Society of London, Series A*, Vol. 307, pp. 55-69.

Ball, K., Farouk, B. and Dixit, V. (1989), "An experimental study of heat transfer in a vertical annulus with a rotating inner cylinder", *International Journal of Heat and Mass Transfer*, Vol. 32, pp. 1517-27.

Bird, R. and Curtiss, C. (1959), "Tangential Newtonian flow in annuli-I unsteady-state velocity profiles", *Chemical Engineering Science*, Vol. 11, pp. 108-13.

Bird, R., Curtiss, C. and Stewart, W. (1959), "Tangential Newtonian flow in annuli-II steady-state pressure profiles", *Chemical Engineering Science*, Vol. 11, pp. 114-7.

El-Shaarawi, M.A.I. and Al-Attas, M. (1992), "Unsteady natural convection in open-ended vertical concentric annuli", *International Journal of Numerical Methods for Heat and Fluid Flow*, Vol. 2, pp. 503-16.

El-Shaarawi, M.A.I. and Khamis, M. (1987), "Induced flow in uniformly heated vertical annuli with rotating inner walls", *Numerical Heat Transfer*, Vol. 12, pp. 493-508.

El-Shaarawi, M.A.I. and Sarhan, A. (1981), "Developing laminar free convection in an open ended vertical annulus with a rotating inner cylinder", *Journal of Heat Transfer*, Vol. 103, pp. 552-8.

El-Shaarawi, M.A.I., Al-Nimr, M.A. and Alyah, M.M.K. (1999), "Transient conjugate heat transfer in a porous medium in concentric annuli", *International Journal of Numerical Methods for Heat and Fluid Flow*, Vol. 9, pp. 444-60.

El-Shaarawi, M.A.I., Al-Nimr, M. and Hader, M. (1995), "Transient conjugated heat transfer in concentric annuli", *International Journal of Numerical Methods for Heat and Fluid Flow*, Vol. 5, pp. 459-73.

El-Shaarawi, M.A.I., Budair, M. and Al-Qahtani, M. (1997), "Turning moment of rotating inner cylinder in the entry region on concentric annuli", *JSME International Journal*, Vol. 40, pp. 67-74.

El-Shaarawi, M. and Alkam, M. (1992), "Transient forced convection in the entrance region of concentric annuli", *International Journal of Heat and Mass Transfer*, Vol. 35, pp. 3335-44.

El-Shaarawi, M. and Al-Nimr, M. (1990), "Fully developed laminar natural convection in open-ended vertical concentric annuli", *International Journal of Heat and Mass Transfer*, Vol. 33, pp. 1873-84.

El-Shaarawi, M. and Negm, A. (1999), "Conjugate natural convection heat transfer in an open-ended vertical concentric annulus", *Numerical Heat Transfer*, Vol. 36, pp. 639-55.

El-Shaarawi, M. and Sarhan, A. (1982), "Combined forced-free laminar convection in the entry region of a vertical annulus with a rotating inner cylinder", *International Journal of Heat and Mass Transfer*, Vol. 25, pp. 175-86.

Floryan, J.M. and Novak, M. (1994), "Free convection heat transfer in multiple vertical channels", *International Journal of Heat and Fluid Flow*, Vol. 16, pp. 244-53.

Hess, C.F. and Miller, C.W. (1979), "Natural convection in a vertical cylinder subject to constant heat flux", *International Journal of Heat and Mass Transfer*, Vol. 22, pp. 421-30.

Holzbecher, M. and Steiff, A. (1995), "Laminar and turbulent free convection in vertical cylinders with internal heat generation", *International Journal of Heat and Mass Transfer*, Vol. 8, pp. 2893-903.

Hwang, J.Y. and Yang, K.S. (2004), "Numerical study of Taylor–Couette flow with an axial flow", *Computers & Fluids*, Vol. 33, pp. 97-118.

Joshi, H.M. (1988), "Transient effects in natural convection cooling of vertical parallel plates", *International Communications in Heat and Mass Transfer*, Vol. 15, pp. 227-38.

Kim, M. and Choi, C. (2005), "The onset of instability in the flow induced by an impulsively started rotating cylinder", *Chemical Engineering Science*, Vol. 60, pp. 599-608.

Kumar, R. (1997), "Three-dimensional natural convective flow in a vertical annulus with longitudinal fins", *International Journal of Heat and Mass Transfer*, Vol. 40, pp. 3323-34.

Mullin, T., Benjamin, B., Schatzel, K. and Pike, E. (1981), "New aspect of unsteady Couette flow", *Physics Letters*, Vol. 83A, pp. 333-6.

Nakamura, H., Yutaka, A. and Naitou, T. (1982), "Heat transfer by free convection between two parallel flat plates", *Numerical Heat Transfer*, Vol. 5, pp. 95-106.

Nelson, D.J. and Wood, B.D. (1989), "Combined heat and mass transfer natural convection between vertical parallel plates", *International Journal of Heat and Mass Transfer*, Vol. 31, pp. 1779-87.

Prasad, V., Kulacki, F. and Kulkarni, A. (1986), "Free convection in a vertical porous annulus with constant heat flux on the inner wall experimental results", *International Journal of Heat and Mass Transfer*, Vol. 29, pp. 713-23.

Reeve, H., Mescher, A. and Emery, A. (2004), "Unsteady natural convection of air in a tall axisymmetric nonisothermal annulus", *Numerical Heat Transfer*, Vol. 45, pp. 625-48.

Rogers, B. and Yao, L. (1993), "Natural convection in a heated annulus", *International Journal of Heat and Mass Transfer*, Vol. 36, pp. 35-47.

Zaki, M., Nirdosh, I. and Sedahmed, G. (2000), "Natural convection mass transfer behaviour of long vertical annuli", *International Communications in Heat and Mass Transfer*, Vol. 27, pp. 435-42.

Corresponding author
Maged A.I. El-Shaarawi can be contacted at: magedas@kfupm.edu.sa